LUND UNIVERSITY

Pharmacokinetic study of a systemically administered novel liposomal Temoporfin formulation in an animal tumor model

Svensson, Jenny; Johansson, Ann; Bendsöe, Niels; Grafe, Susanna; Trebst, Tilmann; Andersson-Engels, Stefan; Svanberg, Katarina

Link to publication

Pharmacokinetic study of a systemically administered novel liposomal Temoporfin formulation in an animal tumor model

Jenny Svensson[a]*, Ann Johansson[a], Niels Bendsoe[b], Susanna Gräfe[c], Tilmann Trebst[d], Stefan Andersson-Engels[a], Katarina Svanberg[e]

[a]Department of Physics, Lund University, P.O. Box 118, SE-221 00 Lund, Sweden
[b]Department of Dermatology, Lund University Hospital, SE-221 85 Lund, Sweden
[c]Research&Development, biolitec AG, Winzerlaer Straße 2, D-07745 Jena, Germany
[d]CeramOptec GmbH, Siemensstraße 44, D-53121 Bonn, Germany
[e]Department of Oncology, Lund University Hospital, SE-221 85 Lund, Sweden

ABSTRACT

M*eso*-tetra(hydroxyphenyl)chlorin (mTHPC) (international generic name Temoporfin) is a potent photosensitizer used for photodynamic therapy (PDT). In this study the pharmacokinetics of a systemically administered novel lipid formulation of Temoporfin in a murine tumor model has been investigated. Fluorescence spectroscopy measurements were performed at several time intervals following drug administration, yielding information on the Temoporfin concentration within excised internal organs as a function of time after injection. Both point-monitoring and imaging setups were used. The acquired fluorescence data were correlated to the concentration of Temoporfin obtained with High Performance Liquid Chromatography (HPLC). There was a significant correlation between the fluorescence methods and HPLC for most organs investigated. The pharmacokinetics of this new liposomal formulation of Temoporfin exhibited a rather flat temporal profile in the time interval 2-8 hours in this study.

Keywords: pharmacokinetics, fluorescence spectroscopy, Temoporfin

1. INTRODUCTION

In the treatment of malignancies with photodynamic therapy (PDT) a photosensitizer is administered to the patient. After some time the drug has accumulated in the tumor tissue and the tumor area is illuminated with light that activates the sensitizer to induce cell death in the tumor. It is preferably to have a short time interval between the drug administration and light illumination. Temoporfin is one of the most potent sensitizers used for PDT[1]. This sensitizer has successfully been intravenously applied in the treatment of various indications, for example head and neck[2], prostate[3] and pancreatic[4] cancer. When using Temoporfin in PDT treatments drug-light intervals of several days are required, and the patients are restricted to limited light exposures. Although Temoporfin is a very potent sensitizer there are some disadvantages for example prolonged skin photosensitivity. The hydrophobic character of the molecule, which leads to the formation of aggregates[5], is another drawback with this substance. When aggregates are formed, low levels of the sensitizer in the target tissue is achieved in relation to the injected dose. This leads to poor sensitizer selectivity and limited PDT treatment outcome[6]. Temoporfin has also been observed to have a short circulation life-time in its monomeric form, which causes problems at the injection site[4,7].

* jenny.svensson@fysik.lth.se; phone +46 462223119; fax +46 462224250

Research groups have tried different delivery vehicles such as liposomes, nano-particles and conjugation to antibodies[8,9] in order to improve e.g. water solubility, tumor selectivity and prolong sensitizer circulation lifetimes. The use of liposomes as sensitizer carrier has been shown to yield higher absolute sensitizer concentration within target tissue, better selectivity and more pronounced PDT effect as compared to its pure analog for other substances, e.g. benzoporphyrin derivative monoacid ring A (BPD-MA)[10].

Using optical methods for tissue characterization and diagnostics in clinic at use have shown promising results. Fluorescence spectroscopy has the advantage of being a non-invasive technique[11]. The spectroscopic information about the state of the tissue is also provided in real time. Different acquisition techniques can be utilized for detection of the induced fluorescence emission. In a point-monitoring setup[12], an optical fiber or thin fiber probe is often used for light delivery and collection. When examining larger areas usually an non-contact imaging mode[13] is preferred. Measurements of photosensitizer levels in tissue can be performed with fluorescence spectroscopy if the sensitizer exhibits fluorescence properties. Temoporfin is characterized by a relatively strong fluorescence yield and red fluorescence is emitted upon excitation with near-ultraviolet light.

The aim of this study is to investigate the pharmacokinetics of Temoporfin incorporated into conventional liposomes based on dipalmitoylphosphatidylcholine (DPPC) following systemic administration. The Temoporfin concentration in a subcutaneously implanted HT29 human colon adenocarcinoma as well as in internal organs in a murine model was measured with both HPLC, which is considered as the gold standard method, and two fluorescence spectroscopy setups. By measuring the Temoporfin concentration with several systems the correlation between fluorescence spectroscopy and HPLC is evaluated in order to investigate whether fluorescence can be used for sensitizer concentration monitoring.

2. MATERIAL AND METHODS

2.1 Sensitizer
Temoporfin is a dark purple, non-hygroscopic, non-solvated crystalline powder, which is soluble in alcohol/acetone/ethyl acetate and practically insoluble in all aqueous media. The single component is of 98% purity with a molecular weight of 680.24 and a fluorescence emission peak at 652 nm. In the novel formulation Foslip (Biolitec Pharma Ltd, Dublin, Ireland) used in this study, the hydrophobic mTHPC is bound to the membrane compartment of the phospholipid bilayer. The liposome formulation is based on DPPC, monosaccharide, water and polyoxyehthylene polyoxypropylene block copolymers[14]. The liposomes were reconstituted and dissolved in 3 ml of sterile water to give a sensitizer concentration of 1.5 mg/ml. Further dilution in 5% aqueous glucose solution provided a sensitizer concentration of 0.075 mg/ml. All compounds were stored at 4°C in the dark.

2.2 Animals
Adult female athymic NMRI nu/nu mice (Harlan Winkelmann GmbH, Germany) were used in this study. All animal experiments were carried out in compliance with the German Animal Protection Act. Six to eight-week old mice, weighing 22-24 g, were inoculated subcutaneously in the left and right hind thigh with a suspension of HT29 human colorectal carcinoma cells (0.1 ml of $8x10^7$ cells/ml in 5 % glucose). When the tumors had reached a diameter of 5-8 mm, and a thickness of 2-4 mm the experiments were performed. The mice were injected with 50 µL of Foslip, corresponding to 0.15 mg Temoporfin/kg, into the lateral tail vein. A dose of 50 mg/kg sodium pentobarbital injected i.p. was used for anaesthesia. Animals were sacrificed 2-8 hours after injection of Foslip and samples of spleen, liver, skin, the two tumors and muscle in each animal were investigated by fluorescence spectroscopy. Following the fluorescence measurements the samples were stored in darkness at -80°C for the HPLC analysis. Three animals with no Foslip injected were used as controls.

2.3 HPLC analysis
All tissue samples were minced by cutting with a scalpel, weighed and freeze dried (Christ Freeze drying system Alpha 1-4 LSC). The resulting powdered tissue was weighed and 10-20 mg was transferred to a 2.0 ml reaction tube after which 1.5 ml of methanol:Dimethyl sulfoxide (DMSO) (3:5, v:v) was added. The samples were immediately mixed for 3 to 5 s periods using a vortex mixer operating at 2,400 rpm and then incubated at 60°C under continuous shaking for at least 12 hours. All samples were spun at 16,000 g in a centrifuge for five minutes. One ml of the supernatant was

transferred to a HPLC vial for subsequent HPLC analysis. The HPLC device had the following specifications; Pump: "System Gold, 126 Solvent Module" Beckman, Autosampler: "Triathlon", Diode Array Detector: "System Gold, Module 168" Beckman and a Fluorescence detector: Shimadzu "RF-10A XL" with interface SS420x. The fluorescence was excited at 410 nm and detected at 653 nm. The separation was carried out on a Merck "LiChroCART 250-4" column with Purospher STAR RP-18 endcapped; 5 µm Guard column: "LiChroCART 4-4" with Purospher STAR RP-18e; 5 µm (Merck) Temperature: 30°C. The mobile phase consisted of acetonitrile: H_2O + 0.1% trifluoroacetic acid (TFA) = 57.5%: 42.5% with a flow rate of 1 ml/min. The tissue concentration of Temoporfin was calculated from a calibration curve constructed by plotting the peak height values of Temoporfin standard solutions versus their concentrations.

2.4 Fluorescence imaging system

The light source used for the imaging setup consisted of an array of light emitting diodes with peak emission at 405 nm. The beam radius of the spot focused onto the organs was 2.5 cm and the irradiance was approximately 30 $\mu W/cm^2$. The fluorescence detection unit consisted of a CCD-camera (C4742-80-12AG, Hamamatsu), a liquid crystal tunable filter having a full-width-half-maximum (FWHM) of 20 nm (LCTF VIS 20-35, Varispec) and a zoom objective lens (50 mm focal length and f/1.8, Nikon). The field of view of the detection system was 3.2 x 4.2 cm. Fluorescence images at 500 and 653 nm, corresponding to wavelengths of tissue autofluorescence and mTHPC fluorescence signals, respectively, were collected. Also background images in the absence of excitation light were acquired using the same wavelengths. For all measurements an exposure time of 3 s was used.

The background was subtracted pixel by pixel from the recorded fluorescence image, followed by normalization with respect to the exposure time. Each fluorescence image was divided by a fluorescence image at 653 nm from a fluorescence standard (USFS 336020, LabSphere, CA, USA) to remove the influence of non-uniform distribution of the excitation light. All fluorescence images were corrected for the difference in relative detection efficiency between the two fluorescence wavelengths (500 and 653 nm) using a calibrated white-light source. The mean and standard deviations of the fluorescence intensity at 500 and 653 nm were calculated within a region of interest (ROI) corresponding to the entire organ. This was performed for each animal and all the individual organs. To estimate the Temoporfin concentration within each organ a fluorescence contrast ratio, R, was calculated;

$$R = \frac{I_a(653) - k \cdot I_c(653)}{I_a(500)} \qquad (1)$$

where $I_a(653)$ and $I_a(500)$ represent the mean value of the intensities within the ROI at 653 and 500 nm, respectively. The terms with the subscript c refer to tissue autofluorescence, calculated as the mean value of the signal from that particular organ of the three control animals. $k = I_a(500)/I_c(500)$ is a scaling factor between the investigated animal and the mean of the three control animals.

2.5 Fluorescence point-monitoring setup

The instrument used for point-monitoring fluorescence spectroscopy is similar to a system described in detail elsewhere[15]. Excitation light at 375 nm was delivered through a 400 µm quartz fiber with a clear cut distal end. Emitted fluorescence was collected through the same optical fiber and reflected laser light was removed by a dichroic beamsplitter (LWP-45-RS396-TU450-700PW1012UV, CVI Technical Optics LTD) and a cut-off filter (RG395, Schott). A spectrometer (USB4000, Ocean Optics) was used to detect the fluorescence signal $F(\lambda)$, which was normalized at 500 nm.

A singular value decomposition (SVD) algorithm was used to fit the data to a set of normalized basis spectra. These spectra consisted of the mTHPC fluorescence signal[16], a fluorescence signal peaking in the blue-green spectral region representing tissue and fiber autofluorescence and assessed as an average of the detected fluorescence signal in each organ of the control animals, and a constant offset representing background in the detection unit. To account for possible changes in tissue blood content and the influence these alterations might have on the autofluorescence spectra[17], a 15-term Fourier series was included in the fit. Eq. (2) gives the detected fluorescence signal as a function of the basis spectra:

$$F(\lambda) = A_{mTHPC} f_{mTHPC}(\lambda) + A_{auto} f_{auto}(\lambda) + A_{offset} + ...$$
$$\left[\omega \sum_{i=1}^{15} \left(B_i \cos\left(\frac{\pi i (\lambda - \lambda_{start})}{\lambda_{end} - \lambda_{start}} \right) + C_i \sin\left(\frac{\pi i (\lambda - \lambda_{start})}{\lambda_{end} - \lambda_{start}} \right) \right) \right], \qquad (2)$$

where the A's, B's and C's are the spectral amplitudes resulting from the fit and the $f(\lambda)$s denote the normalized basis spectra. The fitting was performed in the interval between 500 and 700 nm, but the terms within the square brackets were included only between 500 (λ_{start}) and 640 nm (λ_{end}). The number of components included in the Fourier series was determined by minimizing the error of the fit;

$$E = \left(\sum_i \frac{\left(y_{measured,i} - y_{fit,i} \right)^2}{(n-1)} \right)^{1/2}, \qquad (3)$$

where the summation is taken within the fitting range and n denotes the number of data points in this spectral interval. ω, representing the weighting of the Fourier components in relation to the other factors, was not critical for the performance of the algorithm and was set to 1. Fluorescence spectra were acquired in 1-3 positions in each organ and the SVD algorithm was used to evaluate each spectrum and give a number on A_{mTHPC}. The Temoporfin concentration was quantified by averaging the resulting A_{mTHPC} from the different sites.

2.6 Statistical analysis
The null hypothesis, stating that the four drug-light intervals do not differ, was analyzed with an ANOVA-test for each individual organ. To determine the agreement between the three methods used for assessing the Temoporfin concentration the correlation of the HPLC data, the fluorescence contrast ratio and the Temoporfin fluorescence spectral amplitude was studied. The hypothesis of no correlation for each organ was tested. For all tests, $P<0.01$ was considered significant.

3. RESULTS

Examples of fluorescence intensity images at 653 nm for several excised organs are shown in Figure 1. The images correspond to raw data where no data correction has been performed. Here, a heterogeneous sensitizer distribution can be seen in liver tissue, compared to the more homogeneous distribution in e.g. tumor tissue.
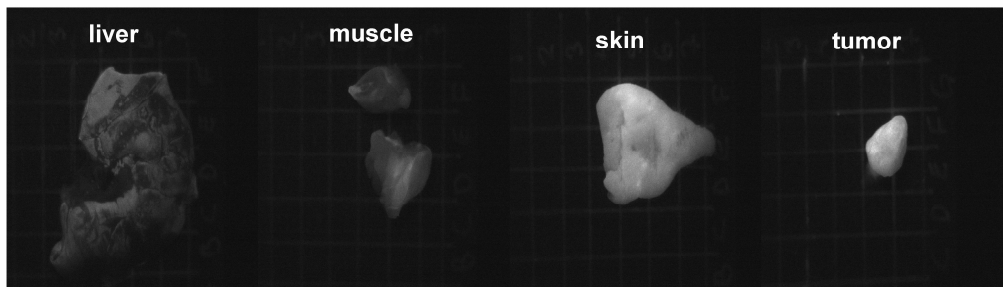

Figure 1. Raw fluorescence intensity images at 653 nm for excised organs. From left to right: liver, muscle, skin and tumor.

3.1 Pharmacokinetics
Figures 2a-b show the Temoporfin concentration in the different organs as a function of drug-light interval investigated by HPLC. Due to the large variation in Temoporfin concentration within the different organs, the results are split in two subfigures for clarity purposes. The average Temoporfin concentration was 0.12 ng/mg in tumor tissue. Only within this tissue the sensitizer concentration showed any significant ($P<0.01$) variation with drug-light interval according to the ANOVA analysis. There was no trace of Temoporfin in any of the control animals. Figure 2c shows the fluorescence contrast ratio, R, as a function of drug-light interval. For the control animals the contrast ratio was close to zero. The

Temoporfin fluorescence amplitude, A_{mTHPC}, evaluated from the point-monitoring data as a function of drug-light interval is shown in Figure 2d. No Temoporfin fluorescence was present in the spectra from any of the control animals. In the figure the average fitting errors, $\hat{E}$, for each organ are shown. For all tissue types, these errors were small compared to the fluorescence signal amplitude. This indicates a good fit. The appearance of Fourier terms mostly reflects the heterogeneous blood distribution within the tissue, and the influence of these terms on the total fit was less than 10% of the autofluorescence component. The error bars in Figure 2a-d indicate the standard deviations arising due to inter-animal variations, whereas for tumor tissue the error bars also partly reflect inter-animal differences in Temoporfin accumulation as each animal had two inoculated tumors. A significant difference in sensitizer concentration over time was indicated through the ANOVA analysis for tumor and skin for the imaging setup. For the point-monitoring data and HPLC data only tumor tissue indicated a significant difference due to drug-light interval. In any of the remaining organs no time-dependence could be detected for both fluorescence methods.
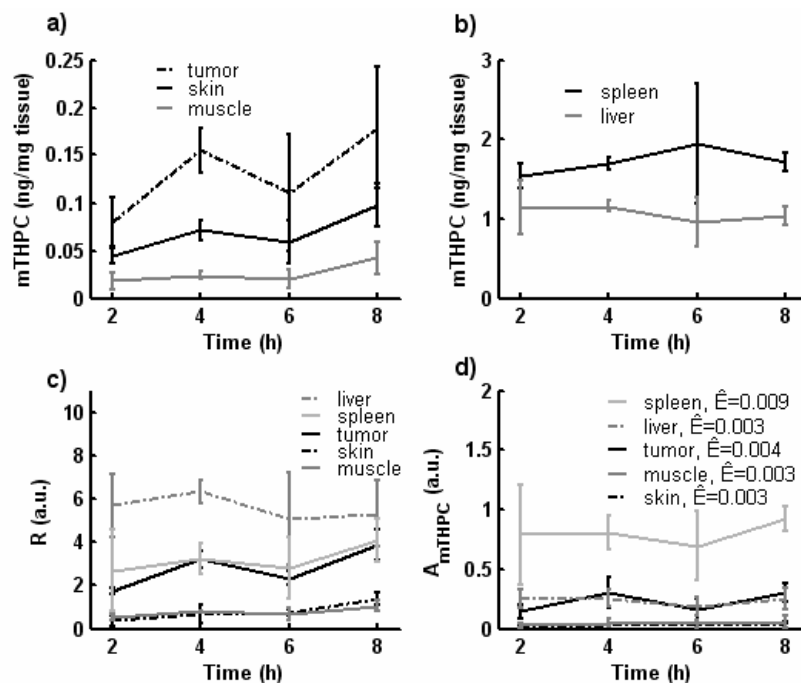

Figure 2. a-b Temoporfin concentration as a function of drug-light interval for the organs investigated by HPLC.
In c and d the fluorescence contrast ratio and the Temoporfin fluorescence amplitude
are seen, respectively, as a function of drug-light interval. Error bars denote ± 1 standard deviation.

3.2 Correlation of HPLC and fluorescence data

One aim of the study was to investigate whether fluorescence spectroscopy measurements could be used in order to determine the absolute sensitizer concentration. This was especially studied by calculating the correlation coefficient between the three methods. In Table 1 the correlation coefficients between each of the three methods for the individual organs are listed. Also the P-values for testing the hypothesis of no significant correlation are given in the table. According to Table 1 there is a significant agreement between the three methods for almost all organs investigated. There was a poor correlation between the optical methods and HPLC for spleen as well as between HPLC and point-monitoring detection of fluorescence for skin.

Table 1. Correlation coefficients between data from each of the three methods used for assessing Temoporfin concentration within the organs. P-values are also given.

	Spleen	Liver	Skin	Tumor	Muscle
HPLC vs fluo. point	0.43 (P=0.15)	0.74 (P<0.01)	0.56 (P=0.04)	0.76 (P<0.01)	0.88 (P<0.01)
HPLC vs fluo. imag	0.53 (P=0.05)	0.85 (P<0.01)	0.70 (P<0.01)	0.87 (P<0.01)	0.78 (P<0.01)
Fluo. imag vs fluo. point	0.67 (P<0.01)	0.78 (P<0.01)	0.75 (P<0.01)	0.63 (P<0.01)	0.70 (P<0.01)

4. DISCUSSION

One of the most potent sensitizers for PDT is the hydrophobic substance Temoporfin. The pharmacokinetics of systemically administration of this sensitizer incorporated into a novel liposomal formulation was investigated in an animal tumor model. Short drug-light intervals in the range of 2 to 8 hours were studied with HPLC, but also with fluorescence spectroscopy as the sensitizer exhibits strong fluorescence. The results demonstrated a rather flat temporal profile of the Temoporfin concentration within the different internal organs. In tumor tissue a significant difference in the concentration depending on drug-light interval was observed for all three methods.

The optical methods were compared to HPLC, which is considered as the gold standard technique for concentration measurements, and data from the three methods were correlated. Within individual organs the different methods showed a relatively good correlation. It was not possible to fit the extraction and fluorescence data from all organs to one single correlation curve. One explanation to this is the difference in the probing volume of the three methods. Extraction results from HPLC represent the average Temoporfin concentration within the entire organ. The fluorescence methods, both imaging and point-monitoring, detect fluorescence only from the most superficial tissue layers. If there would be any variation in Temoporfin concentration due to the depth, this affects the correlation between HPLC and the fluorescence methods.

Another important factor that influences the overall correlation between HPLC and the two fluorescence methods is the difference in optical properties among the tissue types. Optically opaque tissues, such as liver and spleen, result in comparatively lower fluorescence signals than those, for example muscle, characterized by a higher albedo. This demonstrates that it is of importance to take into account the effect the optical properties have on the detected fluorescence signal. Other research groups have performed white-light reflectance measurements probing the same tissue volume as the fluorescence, in order to obtain the tissue optical properties. With this additional information, empirical and theoretical models were used to solve for the intrinsic tissue fluorescence[18,19]. The white-light reflectance measurements yield information on how to receive the fluorescence amplitude and improve agreement between extraction and Temoporfin fluorescence level. Ongoing work within our group has the aim to retrieve the intrinsic fluorescence spectrum where the influences of the optical properties have been removed.

The two fluorescence methods showed similar agreement with HPLC. Even though the optical methods are based on different evaluation principles and have different excitation-detection geometries, the results show that fluorescence can be used as a reasonable estimate of sensitizer concentration. The methods have their individual advantages, for example the imaging setup is less sensitive to heterogeneous uptake of the drug in the organs than the point-monitoring detection setup. In contrast, the point-monitoring detection gives more detailed spectroscopic information compared to the imaging setup. The ideal system would be to image an area and receive information from several spectral bands.

5. CONCLUSIONS

In this study the pharmacokinetics of Temoporfin, incorporated into conventional liposomes at 2 to 8 hours following systemic administration, has been investigated. The pharmacokinetic results with this Temoporfin formulation showed a rather flat temporal profile within the investigated time interval. The results showed that the fluorescence signal could be

used as a reasonable sensitizer concentration estimate within individual homogeneous organs. Finally, it was noted, that the background optical properties of the tissue need to be taken into account to be able to predict the sensitizer concentration with fluorescence spectroscopy methods more accurately.

ACKNOWLEDGEMENTS

REFERENCES

1. S. Mitra and T. H. Foster, "Photophysical parameters, photosensitizer retention and tissue optical properties completely account for the higher photodynamic efficacy of meso-tetra-hydroxyphenyl-chlorin vs Photofrin," *Photochem. Photobiol.* **81**(4), 849-859 (2005)

2. P. J. Lou, H. R. Jager, L. Jones, T. Theodossy, S. G. Bown, and C. Hopper, "Interstitial photodynamic therapy as salvage treatment for recurrent head and neck cancer," *Br. J. Cancer* **91**(3), 441-446 (2004)

3. C. M. Moore, T. R. Nathan, W. R. Lees, A. Freeman, C. A. Mosse, M. Emberton, and S. G. Bown, "Photodynamic therapy for primary prostate cancer - A pilot study using mTHPC," *Br. J. Cancer* **91**, S35 (2004)

4. S. G. Bown, A. Z. Rogowska, D. E. Whitelaw, W. R. Lees, L. B. Lovat, P. Ripley, L. Jones, P. Wyld, A. Gillams, and A. W. Hatfield, "Photodynamic therapy for cancer of the pancreas," *Gut* **50**(4), 549-557 (2002)

5. S. Sasnouski, V. Zorin, I. Khludeyev, M. A. D'Hallewin, F. Guillemin, and L. Bezdetnaya, "Investigation of Foscan interactions with plasma proteins," *Biochim. Biophys. Acta* **1725**(3), 394-402 (2005)

6. J. P. Keene, D. Kessel, E. J. Land, R. W. Redmond, and T. G. Truscott, "Direct detection of singlet oxygen sensitized by haematoporphyrin and related compounds," *Photochem. Photobiol.* **43**(2), 117-120 (1986)

7. M. Triesscheijn, M. Ruevekamp, N. Antonini, H. Neering, F. A. Stewart, and P. Baas, "Optimizing Meso-tetra-hydroxyphenyl-chlorin Mediated Photodynamic Therapy for Basal Cell Carcinoma," *Photochem Photobiol* (2006) doi: 10.1562/2006-07-11-RA-966

8. A. S. L. Derycke and P. A. M. de Witte, "Liposomes for photodynamic therapy," *Advanced Drug Delivery Reviews* **56**(1), 17-30 (2004)

9. Y. N. Konan, R. Gurny, and E. Allemann, "State of the art in the delivery of photosensitizers for photodynamic therapy," *J. Photochem. Photobiol. B.* **66**, 89-106 (2002)

10. A. M. Richter, "Liposomal delivery of a photosensitizer, benzoporphyrin derivative monoacid ring A (BPD), to tumor tissue in a mouse tumor model," *Photochem. Photobiol.* **57**, 1000-1006 (1993)

11. N. Ramanujam, "Fluorescence spectroscopy of neoplastic and non-neoplastic tissues," *Neoplasia* **2**, 89-117 (2000)

12. C. af Klinteberg, M. Andreasson, O. Sandström, S. Andersson-Engels, and S. Svanberg, "Compact medical fluorosensor for minimally invasive tissue characterisation," *Rev. Sci. Instrum.* **76**(3), 034303-034306 (2005)

13. S. Andersson-Engels, J. Johansson, and S. Svanberg, "Medical diagnostic system based on simultaneous multispectral fluorescence imaging," *Appl. Opt.* **33**(34), 8022-8029 (1994)

14. B. Pegaz, E. Debefve, J. P. Ballini, G. Wagnieres, S. Spaniol, V. Albrecht, D. V. Scheglmann, N. E. Nifantiev, H. van den Bergh, and Y. N. Konan-Kouakou, "Photothrombic activity of m-THPC-loaded liposomal formulations: Pre-clinical assessment on chick chorioallantoic membrane model," *European Journal of Pharmaceutical Sciences* **28**, 134-140 (2006)

15. U. Gustafsson, S. Pålsson, and S. Svanberg, "Compact fibre-optic fluorosensor using a continuous wave violet diode laser and an integrated spectrometer," *Rev. Sci. Instrum.* **71**(8), 3004-3006 (2000)

16. M. Angotti, "Etude par spectrometrie de masse des photoreactions laser de sensibilisants colores utilises en therapie photodynamique (PDT)," Thesis. University Paul Verlaine, Metz (2001)

17. W. J. Cottrell, Oseroff, A. R., and Foster, T. H., "Portable instrument that integrates irradiation with fluorescence and reflectance spectroscopies during clinical photodynamic therapy of cutaneous disease," *Rev. Sci. Instrum.,* (2006) doi: 10.1063/1.2204617

18. J. C. Finlay and T. H. Foster, "Recovery of hemoglobin oxygen saturation and intrinsic fluorescence with a forward-adjoint model," *Appl Opt* **44**(10), 1917-1933 (2005)

19. M. G. Muller, I. Georgakoudi, Q. Zhang, J. Wu, and M. S. Feld, "Intrinsic fluorescence spectroscopy in turbid media: disentangling effects of scattering and absorption," *Appl. Opt.* **40**(25), 4633-4646 (2001)